Terra Nova

doi: 10.1111/ter.12186

Debate Article

Plio-Pleistocene increase of erosion rates in mountain belts in response to climate change

Frédéric Herman[1] and Jean-Daniel Champagnac[2]

[1]*Institute of Earth Surface Dynamics, University of Lausanne, Lausanne, Switzerland;* [2]*Free University of Leysin, Leysin, Switzerland*

ABSTRACT

Here, we review an ensemble of observations that point towards a global increase of erosion rates in regions of elevated mountain belts, or otherwise high relief, since the onset of Northern Hemisphere Glaciation about 2–3 Ma. During that period of Earth's history, atmospheric CO_2 concentrations may have dropped, and global climate cooled and evolved towards high-amplitude oscillating conditions that are associated with the waxing and waning of continental ice sheets in the Northern Hemisphere. We argue for a correlation between climate change and increased erosion rates and relief production, which we attribute to some combination of the observed cooling, onset of glaciation, and climatic oscillation at orbital timescales. In our view, glacial erosion played a major role and is driven by the global cooling. Furthermore, analyses of the sedimentary fluxes of many mountain belts show peaks of erosion during the transitions between glacial and inter-glacial periods, suggesting that the variable climatic conditions have also played a role.

Terra Nova, 28: 2–10, 2016

FORUM: The Editors of *Terra Nova* invite readers to contribute to a discussion of this topic on our forum at https://terranovadebates.wordpress.com/

Introduction

Understanding the linkages among climate, erosion and tectonics has been the subject of an active debate over the past three decades, especially since Molnar and England (1990) raised the possibility that climate change, erosion and isostatic rebound might interact in a system of positive feedbacks. One key aspect of that system is that erosion could promote removal of CO_2 from the atmosphere, mainly through silicate weathering of rocks and sequestration of terrestrial organic carbon, to ultimately bring the Earth's climate into an icehouse world (Raymo and Ruddiman, 1992) and, in turn, further enhance erosion. Therefore, central to that discussion has been to establish whether the observed cooling of the Earth's climate during the Late Cenozoic has led to enhanced erosion of mountain belts (Molnar and England, 1990; Zhang *et al.*, 2001; Molnar, 2004; Herman *et al.*, 2013) or not (Willenbring and von Blanckenburg, 2010). Here, we review some of the recent arguments suggesting that both climate and mountain erosion have changed globally during the Plio-Pleistocene and discuss some of the causal implications of the observed temporal connection between the observed changes. Ultimately, we argue that observations are consistent with the hypothesized positive feedback mechanisms between climate and erosion.

Correspondence: Dr. Frédéric Herman, Institute of Earth Surface Dynamics, University of Lausanne, Geopolis, Lausanne CH-1015, Switzerland. Tel.: +4121 692 43 80; e-mail: frederic.herman@unil.ch

Plio-Pleistocene climate change

Using oxygen isotopes, scientists have highlighted a long-term progressive global cooling over the past 50 Ma, punctuated by phases of relatively rapid changes since the Eocene (e.g. Miller *et al.*, 1987; Zachos *et al.*, 2001; Lisiecki and Raymo, 2005, 2007; Fig. 1d). Amongst them, the best-documented change probably corresponds to the onset of Northern Hemisphere Glaciation during the Plio-Pleistocene transition, i.e. since about 3 Ma (Shackleton and Opdyke, 1977; Shackleton *et al.*, 1984; Lisiecki and Raymo, 2005, 2007). A wealth of data now shows that the global climate was vastly different before and after approximately 3 Ma and included a wide array of changes. There was only sparse glaciation in the northern hemisphere and high-altitude regions during the Pliocene, which was followed by an icehouse world since 2.7 Ma, with extensive glaciation that increased towards the present. This is attested by an increase in the variance of the oxygen isotope record (Fig. 1d; e.g. Lisiecki and Raymo, 2005, 2007). Also, the dominant periodicity of the glacial response changed from 41 to 100 ka at the Mid-Pleistocene Transition (MPT), at about 0.9 Ma (Lisiecki and Raymo, 2007). Finally, most recent studies (Fedorov *et al.*, 2013; Martínez-Botí *et al.*, 2015) based on various proxies report that this climate shift was maybe associated with a permanent drop of 50–100 ($\pm$ 100) p.p.m. of atmospheric CO_2 (Fig. 1c; see Fedorov *et al.*, 2013 for a review), which may have played a primary role in the development of large ice sheets in the northern hemisphere (e.g. Crowley and Hyde, 2008; Lunt *et al.*, 2008). It is, however, worth noting that uncertainties associated with current pCO_2 proxies are large and that not all proxies agree, especially going back further in time. For instance, Beerling and Royer (2011) compiled proxies over the entire Cenozoic. They showed that some proxies, but not all,

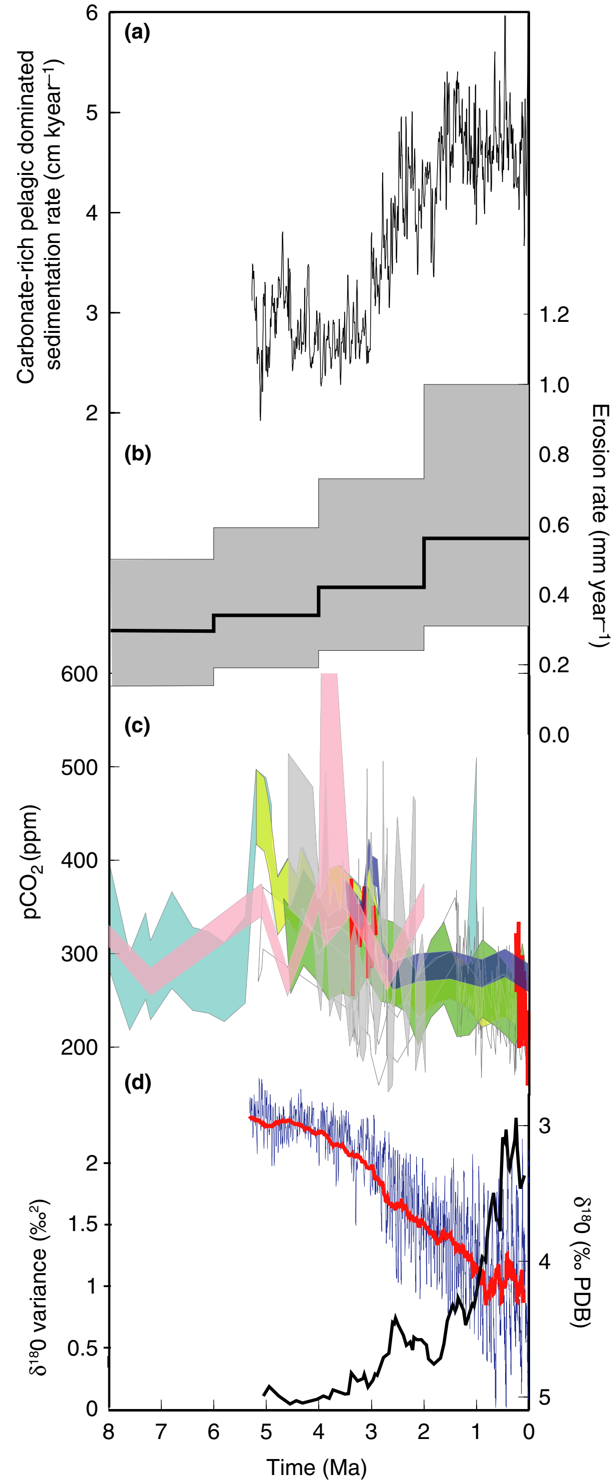

Fig. 1 (a) Global carbonate-rich pelagic sedimentation rate (modified from Lisiecki and Raymo, 2005), which is primarily a function of surface production of microfossil remains, and hence is controlled by the abundance of nutrients as well as dissolved Ca and Si (Raymo *et al.*, 1988). The abundances of these elements are set by the rate of delivery of dissolved material to the ocean (e.g. global chemical weathering supply). (b) Global increase in mountain erosion (modified from Herman *et al.*, 2013). Only regions were resolution in the thermochronometric data enabled erosion rates to be constrained over the last 8 Ma (Fig. 2a) are included, i.e. where the temporal resolution is higher than 0.25 (Herman *et al.*, 2013). The geometric mean and standard deviation (grey area) are estimated from the log-normal distribution of erosion rates over each 2 Ma time interval. (c) Compilation of atmospheric pCO_2 measurements (modified from Fedorov *et al.*, 2013; and Beerling and Royer, 2011). See Fedorov *et al.* (2013) and Beerling and Royer (2011) for the various proxies. (d) Global compilation of oxygen isotope data. The blue line depicts the raw δ^{18}O data compilation (modified from Lisiecki and Raymo, 2005); the red line is a moving average. Black line indicates the variance of the δ^{18}O data over a sliding window of 300 ka.

suggest atmospheric pCO_2 levels that were comparable in the Miocene and Pleistocene, with a warming event at about 4–6 Ma (Fig. 1c).

Finally, the global patterns of winds and precipitation have changed through a progressive equatorward migration of the southern Westerlies and north Atlantic climate belts since the late Pliocene (Cifelli and Glacon, 1979; Dowsett *et al.*, 1996; Heusser *et al.*, 1996; Lamy *et al.*, 1999; Lawrence *et al.*, 2013). The migration of westerly winds is still the subject of discussion, particularly for the northern hemisphere remains (Toggweiler *et al.*, 2006), but if such latitudinal changes in storm-track associated with the westerly winds did occur, they should have played a role in setting erosion rates since the onset of Northern Hemisphere Glaciation. Hulton *et al.* (1994) showed that increased precipitation at about 44°S is necessary to explain the observed ice extent at the Last Glacial Maximum, at about 20 ka, and the Great Patagonia Glaciation, at about 1 Ma. A regional change in ice flux through changes in precipitation would lead to increased ice-sliding velocity. Since glacial erosion is nonlinearly proportional to sliding velocity (e.g. Herman *et al.*, 2015; Koppes *et al.*, 2015), glacial erosion will be sensitive to large changes in precipitation.

Erosion from the sedimentary record

The starting point of the observed increase in erosion rates during Cenozoic cooling, but also the main subject of controversy, is based on estimating the volume of sedimentary sequences in oceanic and continental basins. Molnar and England (1990) initially propounded this hypothesis using the results of Hay *et al.* (1988), who showed that global terrigenous sedimentation on the ocean floor increased by a factor of three during the last 5 Ma. Subsequently, Zhang *et al.* (2001) and Molnar (2004) highlighted that, near continental margins such as on the Mississippi delta and its surroundings, in the North Sea, and in several basins offshore southeast Asia, Nova Scotia, and western Scandinavia, sediment deposition rates all show large increases at about 2–4 Ma (Zhang *et al.*, 2001 for references). Similarly, accumulation rates increased abruptly in late Cenozoic times on continents within, and adjacent to, most of central and Southeast Asia, which represents a significant fraction of Zhang and co-authors' analysis. They showed that accumulation rates may have increased in basins surrounding the Himalayas, Tibet, Tien Shan and Pamir during the Quaternary. Elsewhere, mass accumulation rates show large increases between 0 and 4 Ma in various places such as the European Alps (Guillaume and Guillaume 1982, Kuhlemann *et al.*, 2002), the Amazon Fan (Harris and Mix, 2002), offshore New Zealand (Sutherland, 1996), in the Bay of Alaska (Rea and Snoeckx, 1995), in the Zambezi delta (Walford *et al.*, 2005) and offshore Norway (Anell *et al.*, 2011).

Part of the controversy surrounding the significance of sediment budgets as a proxy for erosion arises from the incompleteness of the record and possible remobilization of previously deposited sediments (e.g. Sadler, 1981; Schumer and Jerolmack, 2009; Sadler and Jerolmack, 2014). More specifically, these authors argue that the global increase may be an observation bias and that erosion rates may have remained globally constant (Willenbring and von Blanckenburg, 2010). Although the existence of a potential observation bias in the sedimentary record is possible, we argue here that it does not disprove the suggestion that erosion rates increased during Cenozoic cooling.

Erosion history from fission track and (U–Th)/He data

Unlike sediment accumulation budgets, thermochronometry provides a first-order estimate of erosion of the bedrock integrated at a Ma timescale. Low-temperature (<300 °C) thermochronometry is suitable for quantifying the time-temperature history of rock cooling within the uppermost 10 km of the Earth's crust (e.g. Reiners and Brandon, 2006). In practice, it consists of measuring apparent ages that represent the time since a rock went through a closure temperature window (Dodson, 1973). Given a temperature field near the Earth's surface, a thermochronometric age can then be converted into an erosion rate integrated over the age time-span (e.g. Braun, 2002; Reiners and Brandon, 2006; Herman *et al.*, 2013; Fox *et al.*, 2014). This means that short-term perturbations and peaks of erosion tend to become smooth, but, more importantly, it cannot lead to an inferred change in erosion rates that does not exist [see Herman *et al.* (2013) for a discussion]. However, potential biases in the interpretation of thermochronometric data may come from multiple sources, e.g. uncertainties in the kinetic parameters, near-surface geotherm, and others, which are in part discussed in Herman *et al.* (2013).

Herman *et al.* (2013) compiled about 18 000 data across the globe for four low-temperature thermochronometric systems [i.e. apatite (U–Th)/He, apatite fission track, zircon (U-Th)/He and zircon fission track], which have closure temperatures of ~70, 110, 180 and 230 °C, respectively (Reiners and Brandon, 2006), and used a formal inversion procedure (Fox *et al.*, 2014) to quantify temporal and spatial variations in erosion rates. This inversion method has the advantages that it allows efficient treatment of a large number of spatially distributed data and it exploits the information contained in both age-elevation profiles and multi-thermochronometric systems strategies.

Thermochronometry can resolve changes in erosion rates only at the time scale provided by the measured age. Therefore, a robust signal of changes in erosion can be inferred only in regions where the ages span the Late Miocene, Pliocene and Pleistocene epochs. Even though the available global dataset comprises ages from a few hundred thousand years to several hundred million years, erosion rates can be extracted only where the ages allow it, i.e. between 8 Ma and today. These mostly correspond to regions where erosion rates are fast, i.e. about 0.35 mm a^{-1} and higher. These inversion results revealed a robust increase in erosion rates in mountain ranges since ca. 6 Ma and most rapidly since 2 Ma (Figs 1b and 2a). The increase in erosion rates is especially well-resolved in the Coast Mountains of British Columbia (Shuster *et al.*, 2005), the central Greater Caucasus (Avdeev and Niemi, 2011), Fiordland New Zealand (Shuster *et al.*, 2011), the western European Alps (Vernon *et al.*, 2008; Fox *et al.*, 2015), northern Patagonia (Thomson *et al.*, 2010), parts of the Himalayas (Thiede and Ehlers, 2013) and the St Elias Range of Alaska (Berger *et al.*, 2008), which is consistent with previous studies in these areas (see Herman *et al.* (2013) for a discussion). Most importantly, all these regions have in common that they have been extensively glaciated during the last 2 Ma. This result implies that glacial and periglacial processes played a role.

Some of the high rates are observed in tectonically active places, and some of the changes may locally be attributed to a simultaneous increase in the rate of crustal accretion (e.g. parts of the Himalayas, Taiwan, Caucasus, Northern Andes or the west coast of the Southern Alps of New Zealand) leading to faster erosion. Nevertheless, the important observation is that the best documented changes are in relatively quiescent places like the Patagonian Andes, western Alps, Coast Mountains of British Columbia and Fiordland, New Zealand where glaciation is a viable explanation for such an important change in erosion.

Unfortunately, fission track and (U–Th)/He thermochronometry do

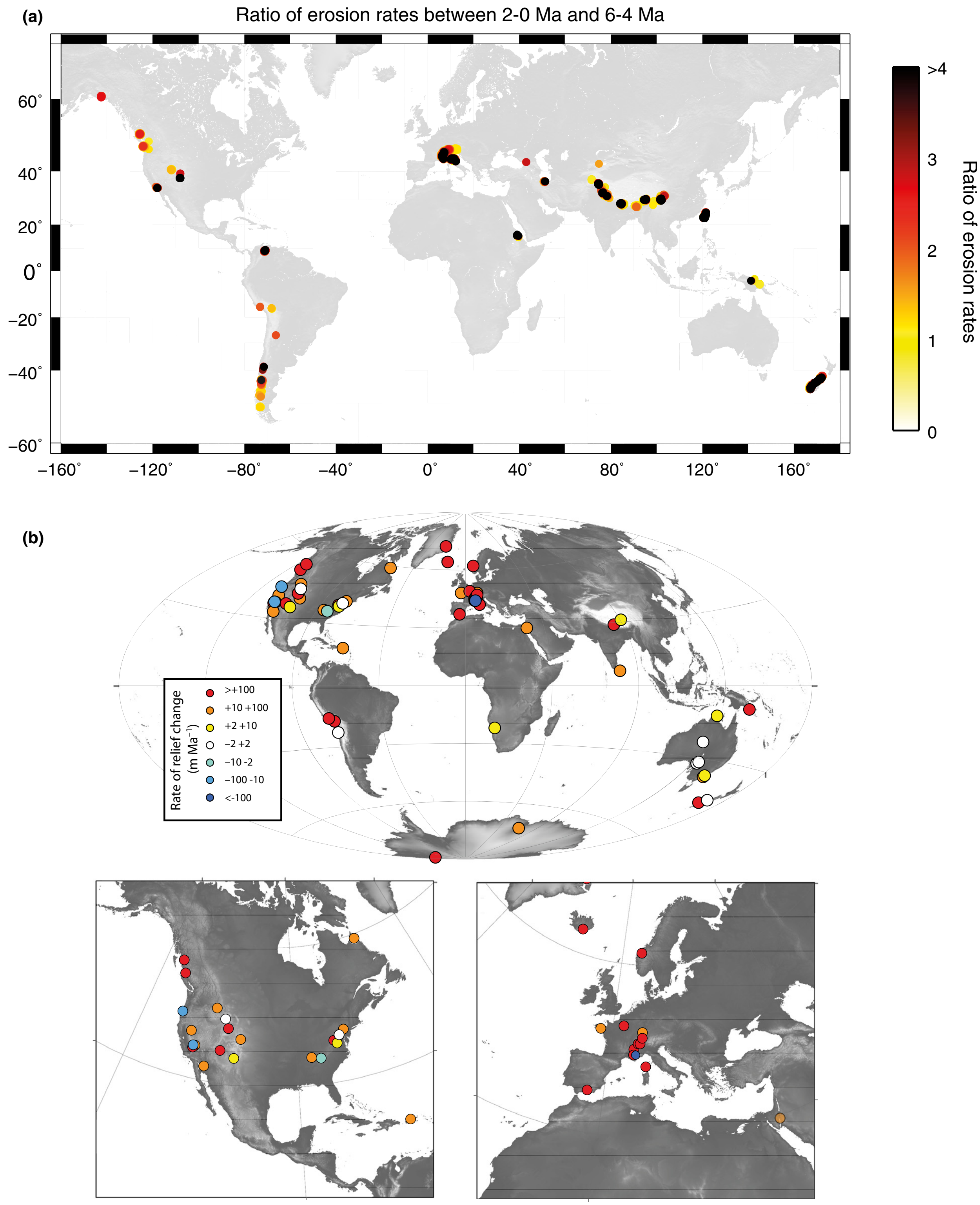

Fig. 2 (a) Change in erosion rates between 0–2 and 4–6 Ma (modified from Herman *et al.* (2013)). (b) Estimates of rates of relief change from a global compilation of studies that focused on relief (modified from Champagnac *et al.* (2014)). Locations and relief-change quantification for the different studies are found in Champagnac *et al.* (2014). Note that most of the studies that explicitly quantify relief change are located in North America and in Europe.

Terra Nova, Vol 28, No. 1, 2–10

not enable us to resolve changes in rates in slowly eroding places such as, for example, western Norway, southern Patagonia, the Rockies or Tien Shan, which has led to controversy (see Molnar, 2004 for references). Even if the increase has been proportionally large in these areas, rates of erosion are too low to exhume rock from sufficiently deep since the change occurred. So the absence of evidence from the inversion of thermochronometric data does not necessarily signify an absence of increase. Furthermore, glaciers have left a distinctive imprint on the morphologies of these landscapes. For example, the substantial landscape modifications that formed the spectacular glacial fjord systems of Norway are thought to have occurred within the Quaternary (e.g. Sejrup *et al*., 1996; Dowdeswell *et al*., 2010; Steer *et al*. 2012). Similarly, Herman *et al*. (2013) did not detect any change in erosion rates in the Tien Shan mountain range, although estimates of palaeo-erosion rates from measurements of ^{10}Be concentration in magnetostratigraphically dated continental sediments (Charreau *et al*., 2011) suggest that erosion rates peaked at about 2 Ma, when the landscape evolved from a fluvial to a glacial morphology at the onset of glaciation. Consequently, the magnitude of increase from the inversion of the thermochronometric data may be seen as a minimum estimate integrated over 2 Ma time intervals.

Erosion history from ^{4}He/^{3}He thermochronometry

Several recent studies have used ^{4}He/^{3}He thermochronometry (Shuster and Farley, 2004) to identify local changes in erosion rates. Unlike (U–Th)/He ages, which are calculated from the total content of radiogenic ^{4}He relative to uranium and thorium, ^{4}He/^{3}He has the advantage that it enables the inference of the spatial distribution of ^{4}He within an apatite crystal. In turn, this spatial distribution can be inverted to constrain the cooling history of rocks between ~80 °C and ~20 °C as they travel towards the surface in response to erosion. Its main advantage is that it provides a higher temporal resolution than (U–Th)/He and fission track dating, though at the expense of considerable experimental effort.

The first application of this method by Shuster *et al*. (2005) in the Coast Mountains of British Columbia concluded that at least 2 km of valley incision has occurred since 1.8 ± 0.2 Ma, implying local erosion rates of at least 5 mm a^{-1}. Subsequently, Shuster *et al*. (2011) used the same approach in Fiordland, New Zealand and inferred that the topography dramatically changed during the last 2 Ma. They also argued that erosion propagates from the low terrain of the mountain belt to its inner part as the landscape switches from a fluvial- to a glacial-dominated morphology, which is consistent with modelling results (Sternai *et al*., 2013; Pedersen *et al*., 2014). Using the same method, Valla *et al*. (2011, 2012) inferred an increase in valley incision in the Rhône Valley, Switzerland, that corresponds to a threefold increase in erosion rates from 0.3–0.5 mm a^{-1} to 1–1.5 mm a^{-1} since about 1 Ma. These results are consistent with other independent studies in other places in the Alps, which were based on cosmogenic burial dating (Hauselmann *et al*., 2007) and the stratigraphic record in the Po plain (Muttoni *et al*., 2003).

Altogether, these studies have identified a significant increase in erosion rates during the Plio-Pleistocene. It is also worth stressing that none of these studies actually sampled the valley bottoms of the large overdeepenings, now filled with sediment or water, in these mountain ranges. It is likely that this part of the landscape experienced even faster glacial incision. For example, the Rhône valley is currently filled with up to 1 km of gravel (Preusser *et al*., 2010), with a gravel-bedrock interface far below the current and Last Glacial Maximum sea level.

Latitudinal variations in erosion rates

The analysis of thermochronometric data also reveals that the increase in erosion rates reaches a maximum at mid-latitudes (Herman *et al*., 2013). Champagnac *et al*. (2012, 2014) also found that relief, changes in relief and the rate of such changes were maximized at mid-latitudes (Fig. 2b). If this pattern is not due to a sampling bias based on the distribution of active collision belts, then latitudinal variations in erosion may be related to adjustments in glacial and periglacial processes. It could be that frost shattering may have played a role because mid-latitudes correspond to regions where temperatures are within the 'frost cracking window' (i.e. between −8 °C and −3 °C, Anderson, 1998; Hales and Roering, 2007; Walder and Hallet, 1985) for the longest period of time. However, documented rates of erosion due to frost shattering vary between 0.1 and <1 mm a^{-1} (e.g. Hales and Roering, 2009; Delunel *et al*., 2010) (which are averaged over relatively large areas), while local rates of glacial incision can be much higher than 1 mm a^{-1}, even when integrated over Ma time scales.

Mid-latitude regions experienced the largest changes between fluvial- and glacial-dominated conditions during the Quaternary. Zhang *et al*. (2001) and Molnar (2004) argued that changes in both the amplitude and frequency of glacial/interglacial cycles might have been responsible for the increase in erosion rates because geomorphic processes never reach equilibrium with climate. Some studies have shown that erosion rates are often highest during the transition from glaciated to ice-free conditions (e.g. Hinderer, 2001; Schlunegger and Hinderer, 2003; Koppes and Montgomery, 2009). The reasons invoked are numerous, including the mismatch or pre-conditioning of landscapes formed by glacial or fluvial processes (Champagnac *et al*., 2009; Norton *et al*., 2010; Pedersen and Egholm, 2013), the evacuation of glacial deposits by rivers (Church and Ryder, 1972), and the effects of periglacial processes during glacial transitions and ice retreat (e.g. Church and Ryder, 1972; Cossart *et al*., 2008; Lebrouc *et al*., 2013). Deglaciation and ice retreat can also lead to an increase in landslide frequency and magnitude (e.g. Holm *et al*., 2004). Frost creep and gelifluxion are also known to increase the mobility of soil/regolith on hillslopes and are most efficient at the transitions between warm and cold conditions (e.g. Anderson, 2002). In addition, rates of glacial carving are largely controlled by ice volume and ice flux (e.g. Anderson *et al.*, 2006; Pedersen and Egholm, 2013; Sternai *et al.*, 2013) and are therefore ruled by cooling and precipitation. This implies that the long-term magnitude of glacial erosion is primarily influenced by changes in amplitude rather than changes in frequency of glacial/interglacial cycles. As a result, the observed erosion increase is most likely related to either, or both, changes in frequency or amplification of glaciations.

Third, it has been shown that relief is higher in glaciated regions, implying that glaciation has led to an increase in local relief since the onset of glaciation. This effect may have contributed to the global increase in erosion in response to climate change (see Champagnac *et al.*, 2012, 2014 for a complete discussion).

Finally, shifts in peak precipitation associated with Westerlies in the southern hemisphere played a role in setting glacial erosion patterns (Herman and Brandon, 2015). At least in the Andes, the position of maximum erosion coincides with the location of maximum precipitation, which follows the southern hemisphere Westerlies during glacial maxima (e.g. Heusser *et al.*, 1996; Lamy *et al.*, 1999; Moreno and León, 2003; Denton *et al.* 2010). The increased precipitation rates at about 44°S during glacial maxima led to enhanced ice flux, increased ice sliding velocity and, in turn, higher glacial erosion rates (Herman and Brandon, 2015). One may speculate that this effect has been operating at a larger scale.

Positive feedback between erosion and climate

The increase in mountain erosion rates implies an increase in sediment fluxes at a global scale, because the relative contribution of mountains to the global production of sediments is about 50% (Milliman and Syvitski, 1992; Larsen *et al.*, 2014; Willenbring *et al.*, 2014), despite covering only about 10% of the emerged land. Furthermore, this glacial erosion may have stimulated a positive feedback in which increased erosion would promote removal of CO_2 from the atmosphere and, in turn, cause further cooling (Molnar and England 1990, Raymo and Ruddiman, 1992). Several mechanisms have been proposed. Most popular is the idea that mechanical erosion in mountains would increase the surface area of fresh mineral, enhance weathering of silicate rocks (e.g. Molnar and England, 1990; Edmond, 1992; Raymo and Ruddiman, 1992) and, in turn, increase pelagic sedimentation rates through the supply of Ca and Si nutrients to the ocean (Raymo *et al.*, 1988; Fig. 1a). Second, some studies have demonstrated that terrestrial organic carbon burial can be very efficient at sequestrating carbon in the ocean, a mechanism that is positively correlated with physical erosion (e.g. France-Lanord and Derry, 1997). In fact, this mechanism has been shown to be far more efficient at withdrawing CO_2 from the atmosphere than silicate weathering, in the Himalayas (Galy *et al.*, 2007), Taiwan (Kao *et al.*, 2014) and globally (Galy *et al.*, 2015).

The case study of the Patagonian Andes potentially raises a new interesting possibility because erosion in this part of the world plays a major role in the production of sediment and dust transported to the Southern ocean. This is the region where variations in iron availability from dust can have the largest effect on Earth's carbon cycle through its fertilizing effect on marine ecosystems (e.g. Martin, 1990; Martin *et al.*, 1990; Martínez-Garcia *et al.*, 2011, 2014), in turn promoting the feedbacks between global climate and erosion. Martínez-Garcia *et al.* (2014) showed that changes in dust flux to the Southern Atlantic Ocean could explain a third of the observed drawdown of atmospheric CO_2 at glacial/interglacial timescales. The production, transport and deposition of fine-grained sediments (dust and/or loess) during glacial periods are documented globally (e.g. Smalley, 1966; Pye, 1995; Jickells *et al.*, 2005). Therefore, a large fraction of these aeolian silts would have been deposited offshore, hence contributing to the global carbon cycle (see Bullard, 2013 for a review).

To sum up, there exist several known possible mechanisms by which erosion can promote a drawdown of atmospheric CO_2. Most research has been invested on the effects of silicate weathering. We realize it may be difficult to isolate and quantify the respective contribution of each component of this system of positive feedbacks, but observations are consistent with the idea that it may have been operating. (Note that if such positive feedbacks have been operating, negative feedbacks are still required to maintain the Earth in a state of equilibrium.) The advent of higher-resolution CO_2 proxies and a continuously increasing number of thermochronometric data and methods (e.g. Herman *et al.*, 2010; Guralnik *et al.*, 2013, 2015) may shed light in the future.

Conclusions

Our current state-of-knowledge suggests that climate progressively cooled, glaciation was further amplified, atmospheric CO_2 levels may have potentially dropped and westerly winds migrated towards the equator since about 3 Ma as a result of Northern Hemisphere Glaciation. The interpretation of the geological, thermochronological and geomorphological data suggests that mountain erosion rates increased over the same time span, with a maximum at mid-latitude, putting further independent constraints on the published sediment accumulation curves and the associated literature.

Acknowledgements

Peter Molnar is thanked for his feedback.

References

Anderson, R.S., 1998. Near-surface thermal profiles in alpine bedrock: implications for the frost weathering of rock. *Arct. Alp. Res.*, **30**, 362–372.

Anderson, R.S., 2002. Modeling the tor-dotted crests, bedrock edges, and parabolic profiles of high alpine surfaces of the Wind River Range, Wyoming. *Geomorphology*, **46**, 35–58.

Anderson, R.S., Molnar, P. and Kessler, M.A., 2006. Features of glacial valley profiles simply explained. *J. Geophys. Res.*, **111**(F1), F01004.

Anell, I., Thybo, H. and Rasmussen, E., 2011. A synthesis of Cenozoic sedimentation in the North Sea. *Basin Res.*, **24**, 154–179.

Avdeev, B. and Niemi, N.A., 2011. Rapid Pliocene exhumation of the central Greater Caucasus constrained by low-temperature thermochronometry. *Tectonics*, **30**, TC2009.

Beerling, D.J. and Royer, D.L., 2011. Convergent Cenozoic CO_2 history. *Nat. Geosci.*, **4**, 418–420.

Berger, A.L., Gulick, S.P.S., Spotila, J.A., Upton, P., Jaeger, J.M., Chapman, J.B., Worthington, L.A., Pavlis, T.L., Ridgway, K.D., Willems, B.A. and McAleer, R.J., 2008. Quaternary tectonic response to intensified glacial erosion in an orogenic wedge. *Nat. Geosci.*, **1**(11), 793–799.

Braun, J., 2002. Estimating exhumation rate and relief evolution by spectral analysis of age-elevation datasets. *Terra Nova*, **14**, 210–214.

Bullard, J.E., 2013. Contemporary glacigenic inputs to the dust cycle. *Earth Surf. Proc. Land.*, **38**, 71–89.

Champagnac, J.-D., Schlunegger, F., Norton, K., von Blanckenburg, F., Abbühl, L.M. and Schwab, M., 2009. Erosion-driven uplift of the modern Central Alps. *Tectonophysics*, **474**, 236–249.

Champagnac, J.-D., Molnar, P., Sue, C. and Herman, F., 2012. Tectonics, climate, and mountain topography. *J. Geophys. Res.*, **117**(B2), B02403.

Champagnac, J.-D., Valla, P.G. and Herman, F., 2014. Late-Cenozoic relief evolution under evolving climate: a review. *Tectonophysics*, **614**, 44–65.

Charreau, J., Blard, P.H., Puchol, N., Avouac, J.P., Lallier-Vergès, E., Bourlès, D., *et al*., 2011. Paleo-erosion rates in Central Asia since 9 Ma: a transient increase at the onset of Quaternary glaciations? *Earth Planet. Sci. Lett.*, **304**, 85–92.

Church, M. and Ryder, J.M., 1972. Paraglacial sedimentation: a consideration of fluvial processes conditioned by glaciation. *Geol. Soc. Am. Bull.*, **83**, 3059–3072.

Cifelli, R. and Glacon, G., 1979. New late Miocene and Pliocene occurrences of Globorotalia species from the North Atlantic; and a paleogeographic review. *J. Foramin. Res.*, **9**, 210–227.

Cossart, E., Braucher, R., Fort, M., Bourles, D.L. and Carcaillet, J., 2008. Slope instability in relation to glacial debuttressing in alpine areas (Upper Durance catchment, southeastern France): evidence from field data and ^{10}Be cosmic ray exposure ages. *Geomorphology*, **95**, 3–26.

Crowley, T.J. and Hyde, W.T., 2008. Transient nature of late Pleistocene climate variability. *Nature*, **456**, 226–230.

Delunel, R., van der Beek, P.A., Carcaillet, J., Bourlès, D.L. and Valla, P.G., 2010. Frost-cracking control on catchment denudation rates: insights from in situ produced ^{10}Be concentrations in stream sediments (Ecrins–Pelvoux massif, French Western Alps). *Earth Planet. Sci. Lett.*, **293**, 72–83.

Denton, G.H., Anderson, R.F., Toggweiler, J.R., Edwards, R.L., Schaefer, J.M. and Putnam, A.E., 2010. The last glacial termination. *Science*, **328**(5986), 1652–1656.

Dodson, M.H., 1973. Closure temperature in cooling geochronological and petrological systems. *Contrib. Miner. Petrol.*, **40**, 259–274.

Dowdeswell, J.A., Ottesen, D. and Rise, L., 2010. Rates of sediment delivery from the Fennoscandian Ice Sheet through an ice age. *Geology*, **38**, 3–6.

Dowsett, H., Barron, J. and Poore, R., 1996. Middle Pliocene sea surface temperatures: a global reconstruction. *Mar. Micropaleontol.*, **27**, 13–25.

Edmond, J.M., 1992. Himalayan Tectonics, Weathering Processes, and the Strontium Isotope Record in Marine Limestones. *Science*, **258**, 1594–1597.

Fedorov, A.V., Brierley, C.M., Lawrence, K.T., Liu, Z., Dekens, P.S. and Ravelo, A.C., 2013. Patterns and mechanisms of early Pliocene warmth. *Nature*, **496**, 43–49.

Fox, M., Herman, F., Willett, S.D. and May, D.A., 2014. A linear inversion method to infer exhumation rates in space and time from thermochronometric data. *Earth Surf. Dyn.*, **2**, 47–65.

Fox, M., Herman, F., Kissling, E. and Willett, S.D., 2015. Rapid exhumation in the Western Alps driven by slab detachment and glacial erosion. *Geology*, **43**(5), 379–382.

France-Lanord, C. and Derry, L.A., 1997. Organic carbon burial forcing of the carbon cycle from Himalayan erosion. *Nature*, **390**, 65–67.

Galy, V., France-Lanord, C., Beyssac, O., Faure, P., Kudrass, H. and Palhol, F., 2007. Efficient organic carbon burial in the Bengal fan sustained by the Himalayan erosional system. *Nature*, **450**, 407–410.

Galy, V., Peucker-Ehrenbrink, B. and Eglinton, T., 2015. Global carbon export from the terrestrial biosphere controlled by erosion. *Nature*, **521**, 204–207.

Guillaume, A. and Guillaume, S., 1982. L'erosion dans les Alpes au Plio-Quaternaire et au Miocene. *Eclogae Geol. Helv.*, **75**, 247–268.

Guralnik, B., Jain, M., Herman, F., Paris, R.B., Harrison, T.M., Murray, A.S., Valla, P.G. and Rhodes, E.J., 2013. Effective closure temperature in leaky and/or saturating thermochronometers. *Earth Planet. Sci. Lett.*, **384**, 209–218.

Guralnik, B., Li, B., Jain, M., Chen, R., Paris, R.B., Murray, A.S., Li, S.-H., Pagonis, V., Valla, P.G. and Herman, F., 2015. Radiation-induced growth and isothermal decay of infrared-stimulated luminescence from feldspar. *Radiat. Meas.*, **81**, 224–231.

Hales, T.C. and Roering, J.J., 2007. Climatic controls on frost cracking and implications for the evolution of bedrock landscapes. *J. Geophys. Res.*, **112**, F02033, doi:10.1029/2006JF000616.

Hales, T.C. and Roering, J.J., 2009. A frost "buzzsaw" mechanism for erosion of the eastern Southern Alps, New Zealand. *Geomorphology*, **107**, 241–253.

Harris, S.E. and Mix, A.C., 2002. Climate and tectonic influences on continental erosion of tropical South America, 0–13 Ma. *Geology*, **30**, 447–450.

Hauselmann, P., Granger, D.E., Jeannin, P.-Y. and Lauritzen, S.-E., 2007. Abrupt glacial valley incision at 0.8 Ma dated from cave deposits in Switzerland. *Geology*, **35**, 143–146.

Hay, W.W., Sloan II, J.L. and Wold, C.N., 1988. Mass/age distribution and composition of sediments on the ocean floor and the global rate of sediment subduction. *J. Geophys. Res.*, **93**(B12), 14933–14940, doi:10.1029/JB093iB12p14933.

Herman, F. and Brandon, M., 2015. Mid-latitude glacial erosion hotspot related to equatorial shifts in southern Westerlies. *Geology*, **43**(11), 987–990.

Herman, F., Rhodes, E.J., Braun, J. and Heiniger, L., 2010. Uniform erosion rates and relief amplitude during glacial cycles in the Southern Alps of New Zealand, as revealed from OSL-thermochronology. *Earth Planet. Sci. Lett.*, **297**(1), 183–189.

Herman, F., Seward, D., Valla, P.G., Carter, A., Kohn, B., Willett, S.D. and Ehlers, T.A., 2013. Worldwide acceleration of mountain erosion under a cooling climate. *Nature*, **504**, 423–426.

Herman, F., Beyssac, O., Brughelli, M., Lane, S.N., Leprince, S., Adatte, T., Lin, J.Y.Y., Avouac, J.-P. and Cox, S.C., 2015. Erosion by an Alpine glacier. *Science*, **350**(6257), 193–195.

Heusser, C.J., Lowell, T.V., Heusser, L.E., Hauser, A., Andersen, B.G. and Denton, G.H., 1996. Full-glacial — late-glacial palaeoclimate of the

Southern Andes: evidence from pollen, beetle and glacial records. *J. Quat. Sci.*, **11**, 173–184.

Hinderer, M., 2001. Late Quaternary denudation of the Alps, valley and lake fillings and modern river loads. *Geodin. Acta*, **14**, 231–263.

Holm, K., Bovis, M. and Jakob, M., 2004. The landslide response of alpine basins to post-Little Ice Age glacial thinning and retreat in southwestern British Columbia. *Geomorphology*, **57**, 201–216.

Hulton, N., Sugden, D., Payne, A. and Clapperton, C., 1994. Glacier modeling and the climate of Patagonia during the last glacial maximum. *Quatern. Res.*, **42**, 1–19.

Jickells, T.D., An, Z.S., Andersen, K.K., Baker, A.R., Bergametti, G., Brooks, N., Cao, J. J., Boyd, P.W., Duce, R.A., Hunter, K.A., Kawahata, H., Kubilay, N., laRoche, J., Liss, P.S., Mahowald, N., Prospero, J.M., Ridgwell, A.J., Tegen, I. and Torres, R. 2005. Global iron connections between desert dust, ocean biogeochemistry, and climate. *Science*, **308**(5718), 67–71.

Kao, S.J., Hilton, R.G., Selvaraj, K., Dai, M., Zehetner, F., Huang, J.C., *et al.*, 2014. Preservation of terrestrial organic carbon in marine sediments offshore Taiwan: mountain building and atmospheric carbon dioxide sequestration. *Earth Surf. Dyn.*, **2**, 127–139.

Koppes, M.N. and Montgomery, D.R., 2009. The relative efficacy of fluvial and glacial erosion over modern to orogenic timescales. *Nat. Geosci.*, **2**, 644–647.

Koppes, M., Hallet, B., Rignot, E., Mouginot, J., Smith Wellner, J. and Boldt, K., 2015. Observed latitudinal variations in erosion as a function of glacier dynamics. *Nature*, **526**(7571), 100–103.

Kuhlemann, J., Frisch, W., Székely, B., Dunkl, I. and Kázmér, M., 2002. Post-collisional sediment budget history of the Alps: tectonic versus climatic control. *Int. J. Earth Sci.*, **91**(5), 818–837.

Lamy, F., Hebbeln, D. and Wefer, G., 1999. High-Resolution Marine Record of Climatic Change in Mid-latitude Chile during the Last 28,000 Years Based on Terrigenous Sediment Parameters. *Quatern. Res.*, **51**, 83–93.

Larsen, I.J., Montgomery, D.R. and Greenberg, H.M., 2014. The contribution of mountains to global denudation. *Geology*, **42**, 527–530.

Lawrence, K.T., Sigman, D.M., Herbert, T.D., Riihimaki, C.A., Bolton, C.T., Martínez-Garcia, A., *et al.*, 2013. Time-transgressive North Atlantic productivity changes upon Northern Hemisphere glaciation. *Paleoceanography*, **28**, 740–751.

Lebrouc, V., Schwartz, S., Baillet, L., Jongmans, D. and Gamond, J.F., 2013. Modeling permafrost extension in a rock slope since the Last Glacial Maximum: application to the large Sechilienne landslide (French Alps). *Geomorphology*, **198**, 189–200.

Lisiecki, L.E. and Raymo, M.E., 2005. A Pliocene-Pleistocene stack of 57 globally distributed benthic d 18O records. *Paleoceanography*, **20**, PA1003, doi:10.1029/2004PA001071.

Lisiecki, L.E. and Raymo, M.E., 2007. Plio-Pleistocene climate evolution: trends and transitions in glacial cycle dynamics. *Quatern. Sci. Rev.*, **26**, 56–69.

Lunt, D.J., Foster, G.L., Haywood, A.M. and Stone, E.J., 2008. Late Pliocene Greenland glaciation controlled by a decline in atmospheric CO_2 levels. *Nature*, **454**, 1102–1105.

Martin, J.H., 1990. Glacial-interglacial CO_2 change: the iron hypothesis. *Paleocanography*, **5**, 1–13.

Martin, J.H., Gordon, R.M. and Fitzwater, S.E., 1990. Iron in Antarctic waters. *Nature*, **345**, 156–158.

Martínez-Botí, M.A., Foster, G.L., Chalk, T.B., Rohling, E.J., Sexton, P.F., Lunt, D.J., Pancost, R.D., Badger, M.P.S. and Schmidt, D.N. 2015. Plio-Pleistocene climate sensitivity evaluated using high-resolution CO_2 records. *Nature*, **518**, 49–54.

Martínez-Garcia, A., Rosell-Melé, A., Jaccard, S.L., Geibert, W., Sigman, D.M. and Haug, G.H., 2011. Southern Ocean dust–climate coupling over the past four million years. *Nature*, **476**, 312–315.

Martínez-Garcia, A., Sigman, D.M., Ren, H., Anderson, R.F., Straub, M., Hodell, D.A., *et al.*, 2014. Iron fertilization of the subantarctic ocean during the last ice age. *Science*, **343**, 1347–1350.

Mercer, J.H. and Sutter, J.F., 1982. Late Miocene—earliest Pliocene glaciation in southern Argentina: implications for global ice-sheet history. *Palaeogeogr. Palaeoclimatol. Palaeoecol.*, **38**(3), 185–206.

Miller, K.G., Fairbanks, R.G. and Mountain, G.S., 1987. Tertiary oxygen isotope synthesis, sea level history, and continental margin erosion. *Paleoceanography*, **2**, 1–19.

Milliman, J.D. and Syvitski, J.P.M., 1992. Geomorphic/tectonic control of sediment discharge to the ocean: The importance of small mountainous rivers. *J. Geol.*, **100**, 525–544.

Molnar, P., 2004. Late Cenozoic increase in accumulation rates of terrestrial sediment: how Might Climate Change Have Affected Erosion Rates? *Annu. Rev. Earth Planet. Sci.*, **32**, 67–89.

Molnar, P. and England, P., 1990. Late Cenozoic uplift of mountain ranges and global climate change: chicken or egg? *Nature*, **346**, 29–34.

Moreno, P.I. and León, A.L., 2003. Abrupt vegetation changes during the last glacial to Holocene transition in mid-latitude South America. *J. Quat. Sci.*, **18**, 787–800.

Muttoni, G., Carcano, C., Garzanti, E., Ghielmi, M., Piccin, A., Pini, R., *et al.*, 2003. Onset of major Pleistocene glaciations in the Alps. *Geology*, **31**, 989–992.

Norton, K.P., Abbuhl, L.M. and Schlunegger, F., 2010. Glacial conditioning as an erosional driving force in the Central Alps. *Geology*, **38**, 655–658.

Pedersen, V.K. and Egholm, D.L., 2013. Glaciations in response to climate variations preconditioned by evolving topography. *Nature*, **493**, 206–210.

Pedersen, V.K., Huismans, R., Herman, F. and Egholm, D.L., 2014. Controls of initial topography on temporal and spatial patterns of glacial erosion. *Geomorphology*, **223**, 96–116.

Preusser, F., Reitner, J.M. and Schlüchter, C., 2010. Distribution, geometry, age and origin of overdeepened valleys and basins in the Alps and their foreland. *Swiss J. Geosci.*, **103**, 407–426.

Pye, K., 1995. The nature, origin and accumulation of loess. *Quatern. Sci. Rev.*, **14**, 653–667.

Raymo, M.E. and Ruddiman, W.F., 1992. Tectonic forcing of late Cenozoic climate. *Nature*, **359**, 117–122.

Raymo, M.E., Ruddiman, W.F. and Froelich, P.N., 1988. Influence of late Cenozoic mountain building on ocean geochemical cycles. *Geology*, **16**, 649–653.

Rea, D.K. and Snoeckx, H., 1995. Sediment fluxes in the Gulf of Alaska: Paleoceanographic record from site 887 on the Patton-Murray seamount platform. *Proceedings of the Ocean Drilling Program. Scientific results*, Vol. 145. Ocean Drilling Program.

Reiners, P.W. and Brandon, M.T., 2006. Using Thermochronology to Understand Orogenic Erosion. *Annu. Rev. Earth Planet. Sci.*, **34**, 419–466.

Sadler, P.M., 1981. Sediment accumulation rates and the completeness of stratigraphic sections. *J. Geol.*, **89**, 569–584.

Sadler, P.M. and Jerolmack, D.J., 2015. Scaling laws for aggradation, denudation and progradation rates: the case for time-scale invariance at sediment sources and sinks. *Geol. Soc. London Spec. Publ.*, **404**(1), 69–88.

Schlunegger, F. and Hinderer, M., 2003. Pleistocene/Holocene climate change, re-establishment of fluvial drainage network and increase in relief in the Swiss Alps. *Terra Nova*, **15**, 88–95.

Schumer, R. and Jerolmack, D.J., 2009. Real and apparent changes in sediment deposition rates through time. *J. Geophys. Res.*, **114**, F00A06, doi:10.1029/2009JF001266

Sejrup, H.P., King, E.L., Aarseth, I., Haflidason, H. and Elverhøi, A., 1996. Quaternary erosion and depositional processes: western Norwegian fjords, Norwegian Channel and North Sea Fan. *Geol. Siliciclastic Shelf Seas*, **117**, 187–202.

Shackleton, N.J. and Opdyke, N.D., 1977. Oxygen isotope and palaeomagnetic evidence for early Northern Hemisphere glaciation. *Nature*, **270**, 216–219.

Shackleton, N.J., Backman, J., Zimmerman, H., Kent, D.V., Hall, M.A., Roberts, D.G., Schnitker, D., Baldauf, J.G., Desprairies, A., Homrighausen, R., Huddleston, P., Keene, J.B., Kaltenback, A.J., Krumsiek, K.A.O., Morton, A.C., Murray, J.W., Westberg-Smith, J. 1984. Oxygen isotope calibration of the onset of ice-rafting and history of glaciation in the North Atlantic region. *Nature*, **307**, 620–623.

Shuster, D.L., Cuffey, K.M., Sanders, J.W. and Balco, G., 2011. Thermochronometry Reveals Headward Propagation of Erosion in an Alpine Landscape. *Science*, **332**, 84–88.

Shuster, D.L., Ehlers, T.A., Rusmoren, M.E. and Farley, K.A., 2005. Rapid glacial erosion at 1.8 Ma revealed by ^{4}He/^{3}He thermochronometry. *Science*, **310**(5754), 1668–1670.

Shuster, D.L. and Farley, K.A., 2004. ^{4}He/^{3}He thermochronometry. *Earth Planet. Sci. Lett.*, **217**(1), 1–17.

Smalley, I., 1966. The properties of glacial loess and the formation of loess deposits. *Nature*, **36**, 476–479.

Sternai, P., Herman, F., Valla, P.G. and Champagnac, J.-D., 2013. Spatial and temporal variations of glacial erosion in the Rhône valley (Swiss Alps): insights from numerical modeling. *Earth Planet. Sci. Lett.*, **368**, 119–131.

Sutherland, R., 1996. Transpressional development of the Australia-Pacific boundary through southern South Island, New Zealand: Constraints from Miocene-Pliocene sediments, Waiho-1 borehole, South Westland. *NZ J. Geol. Geophys.*, **39**(2), 251–264.

Thiede, R.C. and Ehlers, T.A., 2013. Large spatial and temporal variations in Himalayan denudation. *Earth Planet. Sci. Lett.*, **371**, 278–293.

Thomson, S.N., Brandon, M.T., Tomkin, J.H., Reiners, P.W., Vásquez, C. and Wilson, N.J., 2010. Glaciation as a destructive and constructive control on mountain building. *Nature*, **467**, 313–317.

Toggweiler, J.R., Russell, J.L. and Carson, S.R., 2006. Midlatitude westerlies, atmospheric CO_2, and climate change during the ice ages. *Paleoceanography*, **21**, PA2005.

Valla, P.G., Shuster, D.L. and van der Beek, P.A., 2011. Significant increase in relief of the European Alps during Mid-Pleistocene glaciations. *Nat. Geosci.*, **4**, 688–692.

Valla, P.G., van der Beek, P.A., Shuster, D.L., Braun, J., Herman, F., Tassan-Got, L. and Gautheron, C., 2012. Late Neogene exhumation and relief development of the Aar and Aiguilles Rouges massifs (Swiss Alps) from low-temperature thermochronology modeling and ^{4}He/^{3}He thermochronometry. *J. Geophys. Res.*, **117**, F01004, doi:10.1029/2011JF002043.

Vernon, A.J., van der Beek, P.A., Sinclair, H.D. and Rahn, M.K., 2008. Increase in late Neogene denudation of the European Alps confirmed by analysis of a fission-track thermochronology database. *Earth Planet. Sci. Lett.*, **270**, 316–329.

Walder, J. and Hallet, B., 1985. A theoretical model of the fracture of rock during freezing. *Geol. Soc. Am. Bull.*, **96**, 336–346.

Walford, H.L., White, N.J. and Sydow, J.C., 2005. Solid sediment load history of the Zambezi Delta. *Earth Planet. Sci. Lett.*, **238**(1), 49–63.

Willenbring, J.K. and von Blanckenburg, F., 2010. Long-term stability of global erosion rates and weathering during late-Cenozoic cooling. *Nature*, **465**, 211–214.

Willenbring, J.K., Codilean, A.T., Ferrier, K.L., McElroy, B. and Kirchner, J.W., 2014. Short Communication: Earth is (mostly) flat, but mountains dominate global denudation: apportionment of the continental mass flux over millennial time scales, revisited. *Earth Surf. Dyn. Discuss.*, **2**(1), 1–17.

Zachos, J.C., Pagani, M., Sloan, L., Thomas, E. and Billups, K., 2001. Trends, rhythms, and aberrations in global climate 65 Ma to present. *Science*, **292**, 686–693.

Zhang, P., Molnar, P. and Downs, W.R., 2001. Increased sedimentation rates and grain sizes 2-4 Myr ago due to the influence of climate change on erosion rates. *Nature*, **410**, 891–897.

Received 28 August 2014; revised version accepted 29 September 2015